

We are IntechOpen, the world's leading publisher of Open Access books Built by scientists, for scientists

6,900

Open access books available

186,000

International authors and editors

200M

Downloads

Our authors are among the

154

Countries delivered to

TOP 1%

most cited scientists

12.2%

Contributors from top 500 universities



WEB OF SCIENCE™

Selection of our books indexed in the Book Citation Index
in Web of Science™ Core Collection (BKCI)

Interested in publishing with us?
Contact book.department@intechopen.com

Numbers displayed above are based on latest data collected.
For more information visit www.intechopen.com



Nanocomposites Based on Elastomeric Matrix Filled with Carbon Nanotubes for Biological Applications

Stefano Bianco¹, Pietro Ferrario², Marzia Quaglio¹
Riccardo Castagna² and Candido F. Pirri^{1,2}

¹*Center for Space Human Robotics, Fondazione Istituto
Italiano di Tecnologia*

²*Materials and Microsystem Lab (Chilab)-Latemar Unit, Dipartimento di
Scienze dei Materiali ed Ingegneria Chimica, Politecnico di Torino
Italy*

1. Introduction

In recent years nanocomposite materials have prompted huge interest due to their exceptional electrical, thermal and mechanical properties. Carbon nanotubes (CNTs) have become the prevalent constituent in such nanocomposites thanks to their superior mechanical properties and unparalleled thermal and electrical transport capabilities. Carbon nanotube-based nanocomposites have mainly employed a polymer matrix, even if ceramic and metallic materials have also been used. In any case, most composite syntheses have utilized multi-walled carbon nanotubes (MWCNT).

In this chapter, a polydimethylsiloxane/multi-walled carbon nanotube composite is considered and characterized. PolyDiMethylSiloxane (PDMS) is an insulating elastomeric material whose main technological employment had been as a structural material for micro-electrical mechanical systems (MEMS) and microfluidic-based devices. Since 2005, it has been reported that by incorporating carbon nanotubes - especially MWCNTs - in polydimethylsiloxane, the resulting material possess a number of enticing properties that can be successfully harnessed in MEMS technology, both for sensing and actuation mechanisms.

We report on synthesis and morphological characterization with a field-emission scanning electron microscopy (FESEM) analysis, with the optimization of the preparation technique to assess the dispersion of nanotubes within the elastomeric matrix, as well as the affinity between the two constituent phases. The dispersion of the carbon filler and its affinity with the polymer matrix are crucial factors that determine the quality and reliability of nanocomposites. FESEM is an adequate tool for investigating such morphological features.

Owing to the promising applications of PDMS/MWCNT composites in sensing and actuation, we characterized the thermal and electrical behaviour of the material and we demonstrated its applicability for the fabrication of miniaturized devices for bio-analyses. Electrical and thermal characterization was aimed at determining the conductivities of

composites with different nanotube concentrations and what changes are brought about by a rise in temperature. Concerning electrical transport, our data were analyzed by means of the percolation theory. Improvements in thermal transport characteristics present a particular interest for their beneficial effects in the fabrication of devices that need to sustain complex thermal protocols based on fast transitions between different temperatures, like the Polymerase Chain Reaction for DNA amplification.

2. Composite and nanocomposite materials

In the continuing quest for improved performance, currently-used materials frequently reach the limits of their usefulness. Thus researchers are always striving to produce either improved traditional materials or completely new materials. Composite materials are an example of the latter category. Those are multi-phase materials obtained through the artificial combination of different materials in order to attain properties that the individual components by themselves cannot attain.

Three main features characterise composite materials:

- i. the constituents are present in “reasonable” proportions, say greater than 5%;
- ii. the constituent phases display different properties, and hence the composite properties are noticeably different from the properties of the constituents;
- iii. they are produced by intimately mixing and combining the constituents by various means.

The constituent materials are classified into matrix and filler phases. The former is the continuous constituent that is often present in the greater quantity in the composite. The role of the filler, instead, is to enhance the properties of the matrix, including electrical, thermal, and mechanical properties [Chung, 2010]. Usually at least one of the dimensions of the filler is small, say less than 500 μm . In addition, the filler is usually described as being either particulate or fibrous. Particulate fillers have dimensions that are approximately equal in all directions, and are often spherical, cubic or platelet in shape. On the other hand, a fibrous filler is characterised by its length being much greater than its cross-sectional dimension. However, the ratio of length to the cross-sectional dimension, known as the aspect ratio (AR), can vary considerably. Long fibres with high aspect ratios give rise to what are called continuous fibre composites, whereas discontinuous fibre composites are fabricated using short fibres of low aspect ratios. The orientation of the discontinuous fibres may be random or preferred, whereas continuous fibres are usually unidirectional oriented [Matthews & Rawlings, 1999].

Recently much interest has been prompted by a novel class of composite materials, called nanocomposites. Those are composites where one of the phases, namely the filler phase, has at least one dimension of less than 100 nm. Owing to the nanometric scale of the filler, which is also termed “nanofiller”, nanocomposites are endowed with huge interfacial area per volume between matrix and filler. As a result, molecular interactions between the two constituents are much stronger than in composites where the filler has a micrometric scale. Although a variety of nanoparticles, such as nanospheres, have been successfully utilised as a filler material, careful scrutiny has mainly been focused on nanofillers with high aspect ratios. This is down to the fact that fillers characterised by high AR can confer either isotropic or anisotropic properties. In particular, if the filler is randomly oriented in the host matrix the composite will display properties that are independent of the spatial direction under analysis. Otherwise, if the nanocomposite has been devised by inducing a preferred

orientation to the filler, the resulting properties would be heavily dependent on the considered special direction.

Carbon nanotubes have recently emerged as an excellent nanofiller material, thanks to the combination of their small size and particular physical properties [Ajayan & Tour, 2007]. Both single-walled and multi-walled CNTs possess superior thermal and electric properties: they are thermally stable up to 2800 °C in vacuum, their thermal conductivity is about twice as high as diamond, and the electric-current carrying capacity is 1000 times higher than copper wires. Furthermore, theoretical studies carried out on the mechanical properties of CNTs indicate that the elastic modulus is greater than 1 TPa and strengths are 10÷100 times higher than the strongest steel at a fraction of their weight [Harris, 2009]. The exceptional electrical and mechanical properties of CNTs, in particular, have prompted huge interest in the production of nanotube-containing composites materials for electronic and structural applications. In many cases these nanocomposites have employed polymer matrices. By and large, polymers can be easily fabricated without damaging CNTs during processing and they represent a huge class of materials with many interesting properties. In particular, CNTs have been incorporated in polymers with weak mechanical properties and low electric transport. The resulting nanocomposite possess the properties of each component with a synergistic effect: on one hand, the nanotubes serve to provide electrical and thermal conductivity and increase stiffness, strength and toughness; on the other, the polymer matrix allows adequate transfer of loads, reducing slippage between adjacent nanotubes bound by weak Van der Waals interactions [Yakobson et al, 1996].

In particular, some efforts have been recently dedicated to the study of polydimethylsiloxane/carbon nanotubes nanocomposites and such topic will be deepened in the next paragraphs.

2.1 Properties and applications of PDMS/CNT nanocomposite

Polydimethylsiloxane is a silicon elastomer and it is a high performance material on account of its optical transparency, chemical and thermal stability, biocompatibility and mechanical flexibility [McDonalds & Whitesides, 2002]. PDMS is an organosilicon compound, commonly referred to as a silicone, whose chemical formula is $(\text{H}_3\text{C})_3\text{SiO}[\text{Si}(\text{CH}_3)_2\text{O}]_n\text{Si}(\text{CH}_3)_3$, where n indicates the number of repeating monomer units $[\text{SiO}(\text{CH}_3)_2]$ occurrences in the polymer chain. Figure 1 shows the PDMS structure and a 3D representation.

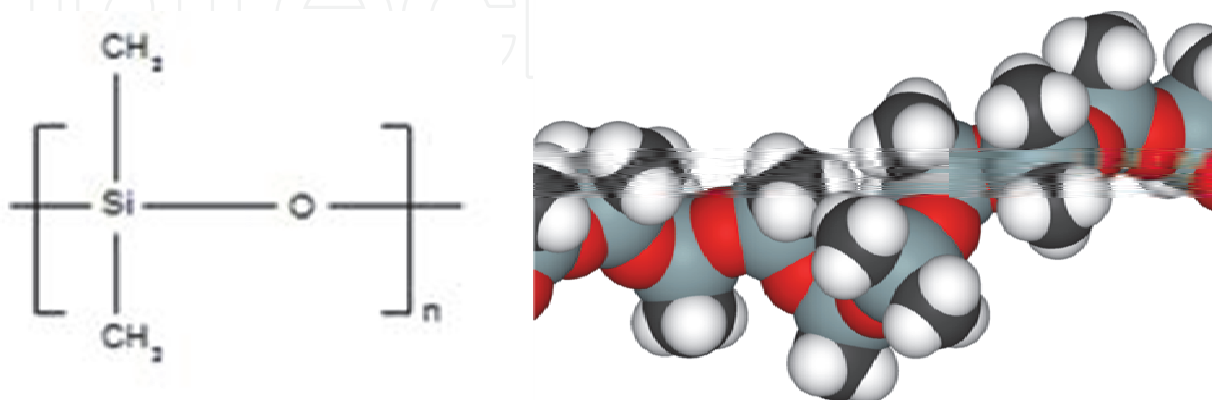


Fig. 1. Chemical formula of PDMS and its 3D structure (from Wikipedia website).

The structure exhibits low intermolecular force between the methyl groups ($-\text{CH}_3$), high flexibility of the siloxane backbone (SiO), high strength of the siloxane bond and a partial ionic nature [Hillborg & Gedde, 1999]. The linear PDMS is liquid at room temperature, because its glass transition temperature $T_g \ll \text{RT}$, in detail $T_g = -127^\circ\text{C}$. Since the methyl groups $-\text{CH}_3$ are characterised by very intense σ bonds, they offer 'protection' to the $-\text{Si-O}$ groups, which are reactive due to their polar nature. Among other things, the methyl groups are also able to rotate around the backbone, thus offering an isotropic protection. [Kim et al, 1999]. Rotation about siloxane bonds in PDMS is virtually free, the energy required for rotation being almost zero [Tobolski, 1960]. This free rotation is reflected in the low glass transition temperature. Its hydrophobic behaviour combined with its low T_g leads to define PDMS as an oil.

The material of interest for MEMS and microfluidic applications is obtained by adding a curing agent (CA) to the PDMS base. The polymer base (also denoted oligomer or pre-polymer) accommodates an unspecified number of vinyl groups, and the curing agent includes at least three silicon hydride bonds for each molecule and some quantity of platinum that acts as a cross-linking catalyst. The addition produces a cross-linking reaction that forms the thermosetting PDMS. Mechanically, this material is referred to as an elastomer. Its viscosity is significantly reduced after cross-linking and the material behaves as a rubber at room temperature.

The cross-linking reaction takes place as the double bond of the polymer base vinyl group ($\text{H}_2\text{C} = \text{CH} -$) is broken, leading to the formation of the $-\text{Si-CH}_2\text{-CH}_2\text{-Si}-$ bond by using one of the $-\text{Si-H}-$ curing agent terminals.

Much interest has been prompted about the surface properties of polydimethylsiloxane. PDMS has a low surface tension, displays a moderate interfacial tension against water, has a high water repellency (i.e. it is hydrophobic), it does not present surface shear viscosity, and has a soft feel [Clarson & Semlyen, 1993]. The adjectives "high", "low", etc. are in comparison to the behaviour of hydrocarbon-based materials. Thus, PDMS has a surface tension lower than almost all organic polymers. One of the very first consequences of the PDMS low surface energy is that whenever it is interfaced with a high energy surface medium such as water a change in the polymer's organization occurs. Lavielle and Schultz [Lavielle & Schultz, 1985] demonstrated that polar groups belonging to PDMS are attracted to the surface by its contact with water. The explanation as to why PDMS is a hydrophobic material was advanced by Khorasani and co-workers [Khorasani et al, 2005], partly derived from L. Franta [Franta, 1988]. According to them, the PDMS structure is a helical one, whose inner part is made of Si-O-Si groups and the outer part consists of methyl groups. The Si-O bond angle is relatively large ($120^\circ\text{-}160^\circ$), which leads to the molecule having a certain degree of flexibility. Hydrophobicity emerges from the different electrochemical nature of the two functional groups.

PDMS is an electrical and thermal insulator, limiting its employment to structural applications that include fluidic channels, valve diaphragms, encapsulating chambers, etc. [Bokobza, 2004; Demir et al, 2005]. Carbon nanotubes can confer to it a significant enhancement of the electrical, thermal and mechanical properties. The addition of CNTs above a critical threshold value reduces the resistivity of the composite by several orders of magnitude, and it has been reported that thermal conductivity is enhanced by 65% with a 4 wt% multi-walled nanotube loading [Liu et al, 2004]. Moreover, it has been shown that the addition of 2 wt% single-walled nanotubes to PDMS produces a 203% improvement in elastic modulus and a 154% in yield strength over the pure polymer [Moniruzzaman et al,

2007]. PDMS/CNT nanocomposites show a number of notable properties that could be easily exploited in micro-electro mechanical systems. However, to date, very few works have been published regarding the employment of PDMS/CNT composites in MEMS technology. PDMS/CNTs composites have mainly been used as strain gauges and pressure nanosensors. It is known that such composites are piezoresistive materials, i.e. materials that change their nominal resistivity due to applied mechanical stress. Although the gauge factor (GF) ($\Delta R/R$) is not high compared with other materials, the sensitivity of the composite to pressure is expected to be quite large due to its large Young's modulus [Wu et al, 2009]. Under an externally applied pressure, the relative resistance measured along the same direction increases, and this effect is stronger if the concentration of carbon nanotubes is low [Hu et al, 2008]. Since most piezoresistive materials are also sensitive to temperature, it is important to characterise the temperature coefficient of resistivity (TCR) of PDMS/MWCNT. As reported by Xu and Allen [Xu et al, 2010] the measured TCRs are much smaller than their piezoresistive coefficients, less than $0.005\text{ }^{\circ}\text{C}^{-1}$. This aspect indicates that the resistivity does not vary significantly under normal working conditions. The piezoresistive properties and low TCRs have been successfully capitalised on the fabrication of strain gauges. For example, PDMS/MWCNT nanocomposites have been utilised to determine the displacement of cantilevers or micro-beams, which are important components in MEMS. The amount of displacement is transduced by a change of resistance of the composite that in turn causes a voltage imbalance in a Wheatstone bridge. Moreover, Kang and colleagues (Kang et al, 2006) have extended the composite sensor to a long strip, named "neuron sensor". They suggested that a neural system in the form of a grid could be attached to the surface of a structure to form a sensor network, enabling structural health monitoring.

On account of the electrical conductivity of PDMS/MWCNTs composites, it has been feasible to create tactile sensors through an array of intertwined capacitors [Engel et al, 2006]. The electrodes of the capacitors are made of PDMS/MWNT composite. The network is composed of two layers of elastomer oriented orthogonal to each other. If pressure is applied, the electrodes on which the external force is addressed will get closer to their respective electrodes on the bottom matrix, thus increasing their capacitance.

Together with sensing properties, actuation characteristics were studied as well. Actuator materials have the faculty of changing their physical dimensions in response to external stimuli and transfer a variety of forms of energy into mechanical work. With regard to their corresponding energy supplies, they can be classified into electrical, thermal, pneumatic and optical actuators [Kovacs, 1998]. Various studies have revealed that when MWCNTs were embedded into a polymer matrix, including PDMS, the nanocomposites experienced either contractive or expansive actuation under light illumination determined by the nanotubes concentration and alignment. In particular, PDMS/MWCNT composites showed structural expansion in response to light under small pre-strains. Under large pre-strains, they showed instead structural contraction in response to light [Ahir & Terentjev, 2005; Ahir et al, 2006]. These properties have not been widely turned to advantage. PDMS/MWCNT composite is a good candidate material for optical actuation, which brings distinctive advantages such as wireless actuation, remote controllability, electromechanical decoupling, low noise, elimination of electrical circuits and higher-level integrity [Lu & Panchapakesan, 2007]. Those composites could therefore be useful in nanoscale devices whereby incorporating batteries is not feasible and the only form of energy is external light. Such devices are said to be working on energy harvesting (or scavenging). In addition, it has been shown that the

photomechanical actuation of PDMS/MWCNT composites can be integrated with microelectromechanical technologies to develop CNT-based micro-optomechanical systems (CNTMOMS) [Lu & Panchapakesan, 2005; Lu & Panchapakesan, 2006]. Another innovative form of optical actuation and energy harvesting application has been figured out by D. Okawa and colleagues [Okawa et al, 2009]. The Zettl's group availed itself of recent studies performed on vertically aligned carbon nanotube forests (VANTs). This material exhibits high absorption of visible light (99.9%) that is quickly then turned into heat through electron relaxation, thus rendering VANTs optimum heat switches. Heating up VANTs gives rise to the formation of surface tension gradients at the interface with a liquid in contact with the nanotubes. Owing to the optical transparency of polydimethylsiloxane, to its perfect adhesion with VANTs and to its density (similar to water), VANTs were embedded in the elastomer. By focusing light in appropriate regions of VANTs, optically induced thermal surface tension gradients propelled the structures (PDMS+VANTs) either in linear or circular paths, depending on the device design.

The tailoring of the aforementioned material properties gives to the PDMS/CNT nanocomposite a multipurpose feature. Such increased properties can find a fruitful application in the fabrication of a new generation of biodevices. The improvement of thermal transport properties, in particular, can increase the efficiency and selectivity of polymer-based devices for Polymerase Chain Reaction (PCR). The efficiency and selectivity of PCR is strictly related to the execution of fast transitions among the three temperatures required by the thermal protocol. Miniaturized devices with reduced mass, as in Micro-Total Analysis Systems for DNA amplification, exhibit a lower thermal inertia than traditional bench-top instruments, increasing the amplification efficiency. The main research goal lays in giving life to a new generation of small, portable and fast devices for applications ranging from clinical medicine, to genetic disease diagnostics and forensic science.

In that scenario, the development and study of innovative materials and technological processes gained a crucial importance. On the first works silicon and glass were used, being their micro-technology well developed and robust compared to any other material [Reyes et al, 2002]. More recently, many efforts were spent in exploring the use of polymers as PDMS, PolyMethylMethAcrylate (PMMA), PolyCarbonate (PC) and Cyclic-Olefine-Copolymer (COC), which are low cost, easy to be manufactured, optically transparent and biocompatible [Zhang et al, 2006; Zhang & Xing, 2007].

Despite the promising characteristics of polymers, their low thermal conductivity is the main problem to face to design disposable PCR Lab-On-a-Chips (LOCs), being rapid temperature transitions difficult to achieve. Till now, four main strategies have been proposed to overcome this problem [Zhang et al, 2006; Zhang & Xing, 2007; Wu et al, 2009]: (i) reducing the thermal inertia of the device by reducing its dimensions; (ii) using optimized thermocyclers; (iii) performing dynamic PCR reactions; (iv) fabricating integrated heaters.

Polymeric composites, in the case of filling with thermally conducting nanomaterials, can show a dramatic improvement in thermal response with respect to traditional polymers. In that field, the improvement in reaction efficiency using PDMS/CNT nanocomposite was recently demonstrated by our group [Quaglio et al, 2011]. Moreover, combining the obtained thermal performance with the improved electrical conduction properties and some of the other material characteristics like the wettability behaviour, it is possible to design innovative all-polymeric devices with integrated heaters, opening new attractive scenarios in bioscience.

3. Nanocomposite preparation and morphological characterization

Reading through the obtainable literature on PDMS/CNT composites, it is immediately noticeable that the ways of preparing PDMS/MWCNT composites are as numerous as the research groups who have published works on the composite's properties. With the exception of a few overly complicated techniques that include demanding and multi-step functionalizations of nanotubes, all preparations require four main “ingredients”: the PDMS polymer base (PB), the curing agent (CA) that activates the cross-linking reaction, CNTs and finally a solvent for nanotube dispersion within the polymer matrix. The ratio of CNTs to PDMS elastomer is chosen depending on the desired application and performance of a device. In the case of uninvolved conductors for capacitive sensors or resistive heaters, a large quota of carbon nanotubes may be added in order to increase the conductivity of the composite. On the other hand, strain and force sensitive sensors call for lower loading of nanotubes to enhance the sensitivity. In all cases, satisfactory dispersion of carbon nanotubes is an essential prerequisite. Here the adjective “satisfactory” denotes a level of dispersion whereby there are no macroscopic bundles or clusters of nanotubes. The level of homogeneity attained in the nanocomposite is usually verified with electron microscopy observations. Electron microscopy could also shed light on several other morphological features of PDMS/MWCNT composites, including a qualitative assessment of the grade of affinity between carbon nanotubes and polymer matrix.

3.1 Matrix characteristics

The chosen PDMS was the Sylgard® 184 Silicone Elastomer Kit, from Dow Corning (USA), comprising a liquid base oligomer (dimethylsiloxane with the vinyl functional group, $\text{SiH} = \text{CH}_2$) and a curing agent (pre-mixture of a platinum complex and copolymers of methylhydrosiloxane and dimethylsiloxane, SiH). When mixing base and curing agent at a typical ratio of ten parts base to one part curing-agent by weight, the catalyst promotes a hydrosilylation reaction between base and curing agent [Xia & Whitesides, 1998]. Its main characteristics can be listed as follows:

- it exhibits a good thermal stability, up to 190°C in air;
- its mechanical properties can be adjusted by modifying the mixing ratio between PB and CA or the polymer base molecular weight. Different stiffness levels, different elastic modulus and adhesion energy are thus obtained;
- its low viscosity makes casting into moulds down to few hundred microns feasible and it can be spinned to fill mould voids deeper than $5\text{ }\mu\text{m}$;
- it is rather effortless to remove the cross-linked polymer from moulds;
- it is chemically inert;
- it is isotropic and homogeneous;
- it is an electrical insulator with a break-down voltage of about $2 \times 10^7\text{ V/m}$;
- it is not toxic or cancerous or in any way harmful to human beings and the environment;
- the high flexibility of the backbone allows the permeability of many gases and vapours [Hillborg & Gedde, 1999];
- hot, damp environments, such as superheated steam, are very detrimental to PDMS integrity. That is due to the partially ionic nature of the siloxane backbone that has a tendency to suffer from nucleophilic or electrophilic attack resulting in a susceptibility to hydrolysis by water [Clarson & Semlyen, 1993].

3.2 Filler characteristics

The multi-walled carbon nanotubes used in this work for nanocomposite preparation were supplied by Nano Carbon Technologies Co. Ltd (Japan). They were synthesised through a floating reactant method. This is a particular CVD technique that allows thorough dispersion of the hydrocarbon in the catalytic particle solution. The synthesis requires an organo-metallic compound (ferrocene) as a catalyst precursor, an organic solvent (toluene) as a carbon feedstock and hydrogen as a carrier gas. Toluene and ferrocene are fed into the reactor through a microfeeding pump and temperature is raised at 1200 °C. Then a thermal treatment is accomplished for 30 min in high purity argon at 2600 °C. The thermal treatment, or thermal annealing, is used to remove residual metal catalyst particles. It has been experimentally shown that annealing catalytically-produced MWCNTs at graphitization temperatures (1600÷3000 °C) has the effect of not only removing the catalyst impurities but also of improving the structural quality of the tubes by turning them into straight “threads” [Musso et al, 2008]. Table 1 summarises the structural and physical properties of the as-prepared and annealed CNTs, as reported previously [Kim et al, 2005]. In this work, annealed MWCNTs were used.

	As-grown nanotube	Annealed nanotube
Interlayer spacing d_{002} [nm]	0.342	0.3385
Diameter [nm]	20÷70	20÷70
Aspect ratio	>100	>100
Volume density [g/cm ³]	0.005	0.005
Real density [g/cm ³]	1.89	2.1
Specific surface area [m ² /g]	28	28
Temperature of oxidation [°C]	560	600
Metal impurity	14wt%	<450 ppm

Table 1. Characteristics of the nanotube used in this study, as reported previously [Kim et al, 2005]. Interlayer spacing was estimated by XRD, diameter and length of the tube by FESEM analyses, volume density by tapping method, real density by a pycnometer, specific surface area by BET (N₂ physisorption), temperature of oxidation by TGA and metal impurity by X-ray fluorescence spectroscopy.

3.3 Nanocomposite preparation

Different preparation methodologies were suited for material preparation, especially depending on the filler content. Samples with low loading concentration were fabricated with the most straightforward technique (namely “A”). The step-by-step procedure is as follows:

1. the nanotubes and the PB quantities are weighted via digital balance and preliminary mixed with a metallic spatula;
2. the mixture is poured into an agate mortar and further mixing occurs. Blending is achieved through a pestle and in order to ensure good dispersion of nanotubes, it is advisable to apply a persistent shear force;
3. the mélange is left to degas for 24 hours;
4. the curing agent is added in a 10:1 ratio to PB, followed by long hand stirring with a pestle;
5. second degassing;

6. transfer everything into previously rinsed moulds and let two to three hours to go by, then heat up the oven at 85 °C and put the moulds inside; consider that samples with a low CNTs concentration will just demand twenty minutes to cross-link, while those with higher concentrations (>1.0 wt%) could necessitate up to two hours.

Given the low concentration of carbon nanotubes relative to the polymer matrix, the consistency of the mixture prior to casting is akin to pure PDMS's. Thence, casting into moulds is performed by simple dripping.

The second preparation method, which will be hereafter denoted by "B", is among the simplest and quickest when it comes to fabricating samples with high concentration of nanotubes (>2 wt%) and foresees a pre-dispersion of nanotubes in a solvent, as suggested for example by L. Bokobza [Bokobza, 2009]. The preparation works as follows:

1. the nanotubes were mixed with isopropanol in an open container; the amount of solvent employed rendered the mixture fluid;
2. the PDMS oligomer was mixed with an excess of isopropanol so that the resulting consistency is similar to that of the curing agent;
3. the two mixtures were sonicated together for hours;
4. solvent was let partially evaporate under chemical hood;
5. the procedure follows as from point 2 in preparation "A".

It is known from literature that the presence of nanotubes inside the matrix partially hinder the reticulation of the polymer [Xu et al, 2008]. Thus, significantly longer times are needed for the preparation "B", because both of the higher number of preparation steps and the need for a longer reticulation time.

3.4 Morphological analysis

A morphological characterization through Field Emission Scanning Electron Microscopy was performed to evaluate the dispersion degree of the filler inside the polymeric matrix. It is well known that a uniform dispersion of the filler is a big issue, since nanotubes tend to form agglomerate because of the Van der Waals forces acting on the wide exposed surface of the nanostructures. Thus, CNTs are usually in form of bundles that need to be broken by applying a strong shear force. FESEM analysis is a powerful tool to evaluate the efficiency of the above-reported preparation procedures.

It was decided to carry out the FESEM analysis on cross-sections of PDMS/MWCNT nanocomposites. After the samples had cross-linked and been extracted from moulds, a 1 mm-thick slice was cut out from each sample with a cutter blade. The cross-sections were then coated with chromium to avoid charging during electron irradiation and mounted on the instrument's sample holder.

The first set of pictures (Figure 2) is a collection of images taken from samples with increasing CNTs concentration, all obtained with the same magnification (5.00 kx). For low CNTs concentrations (<2 wt%) the samples are to all intents and purposes non-conductive, inasmuch as the nanotubes are far apart or form unconnected bundles. As the concentration is increased, the nanotubes give rise to a sort of conductive path more (4 wt%) or less (3 wt%) homogeneous. The sample with a CNTs concentration of 0.5 wt% was fabricated in line with preparation "A". The cracks present in some images do not belong to the sample but rather to the chromium coating.

The use of multiple steps of mixing, including sonication, present in preparation "B" have made it possible to achieve samples with better levels of dispersions, as it has just been

shown in Figure 2 (d) and (e). In spite of the lower nanotube content, the 3 wt% sample exhibit small bundles (the bright circular spots) that are not present in the 4 wt% sample. As it has been mentioned above, the improved dispersion has the disadvantage of a very time-consuming preparation because of slow cross-linking.

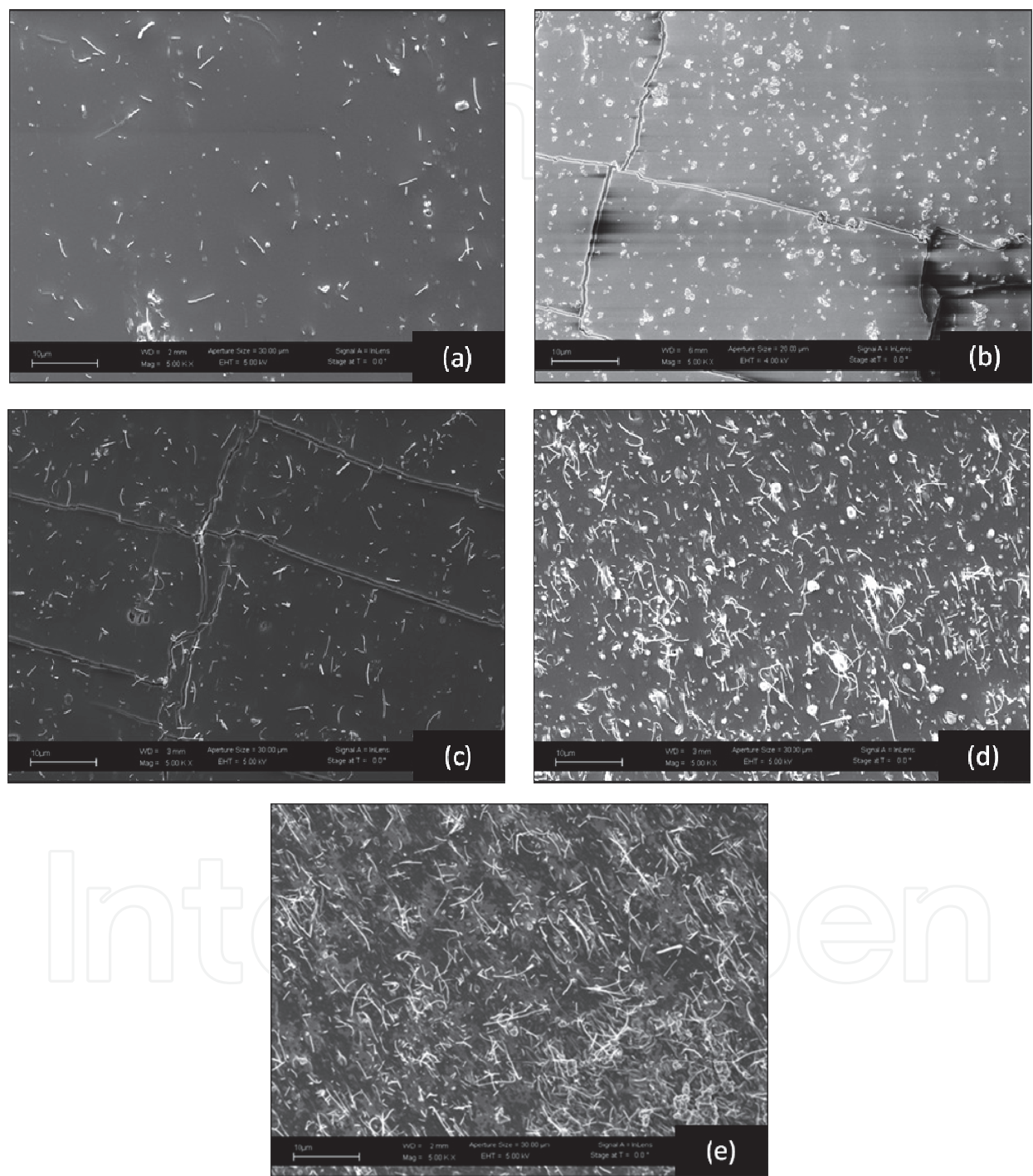


Fig. 2. FESEM images of nanocomposites with a concentration of nanotubes equal to (a) 0.5 wt% (prep. "A"), (b) 1.0 wt% (prep. "A"), (c) 2.0 wt% (prep. "B"), (d) 3.0 wt% (prep. "B") and (e) 4.0 wt% (prep. "B"). All images were shot with a magnification factor of 5000. Some of the visible cracks are not due to the composite but rather relate to the chromium layer.

Notwithstanding the use of solvents and the sonicator, the presence of nanotube clusters is ubiquitous at small scales. Indeed, as shown in the collection of pictures listed in Figure 3, nearly all the samples present regions where nanotubes are scant alongside regions where their concentration is greater. The clusters of carbon nanotubes visualised in Figure 3 are nonetheless small – of the order of just few microns - compared to the dimensions of the nanocomposites that develop at the millimetre scale; the CNT bundles exhibited by the samples fabricated with preparation “B” are the smallest achievable by hand mixing and sonication combined, and represent a limit of this technology.

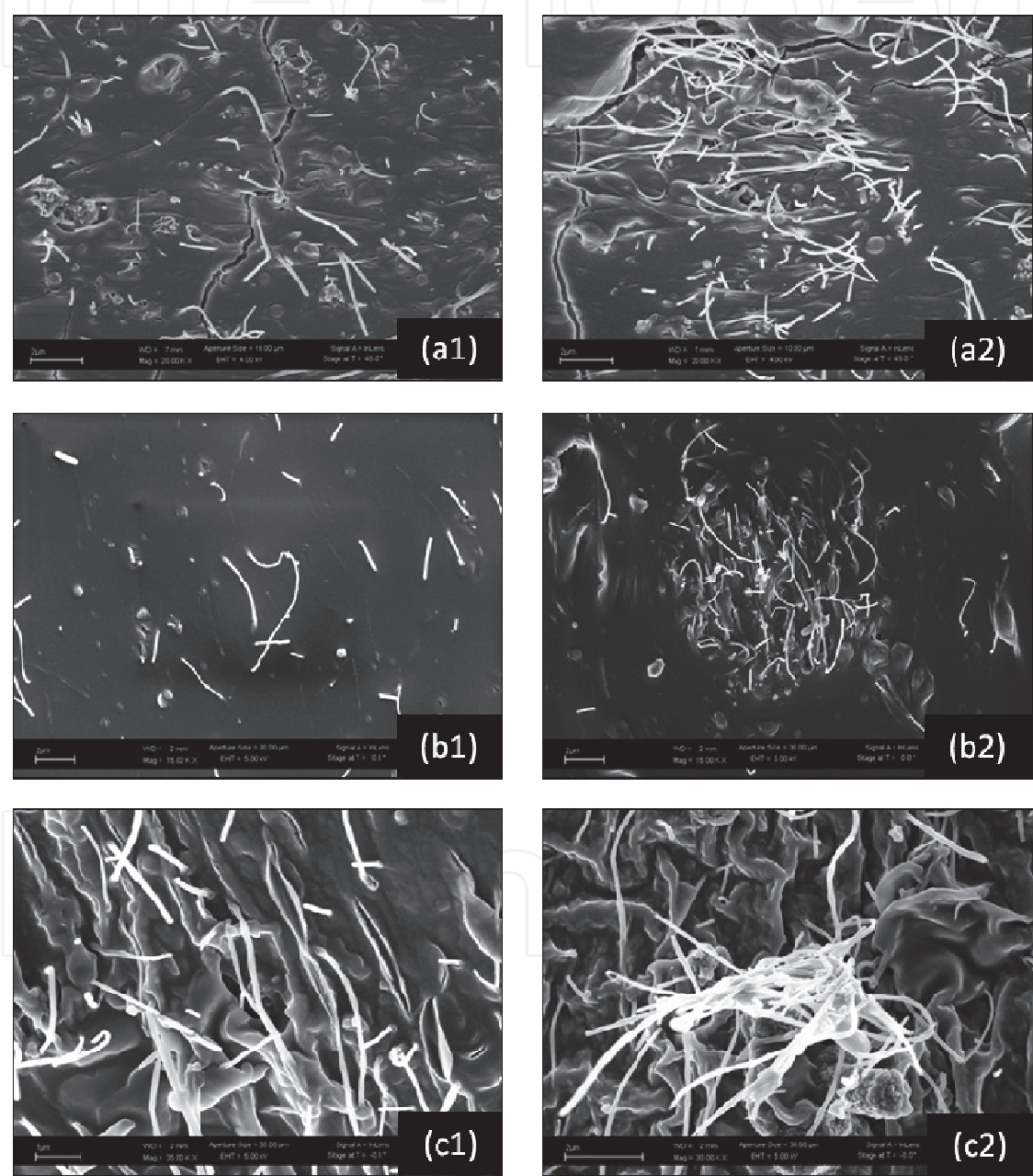


Fig. 3. The left column (1) of this matrix of images refers to regions where different samples display a relatively low concentration of carbon nanotubes. The right column (2), on the other hand, concerns regions where the CNTs concentration is higher. (a) 2 wt% (prep. "A"), 20.00 kx; (b) 0.5 wt% 15.00 kx (prep. "A"); (c) 4 wt%, 30.00 kx (prep. "B").

Furthermore, the hand mixing performed through the mortar was the essential process that ultimately ensured limited dimensions of the clusters. As a matter of fact, attempts to prepare composite using only the sonicator were tried out and Figure 4 illustrates one of those.

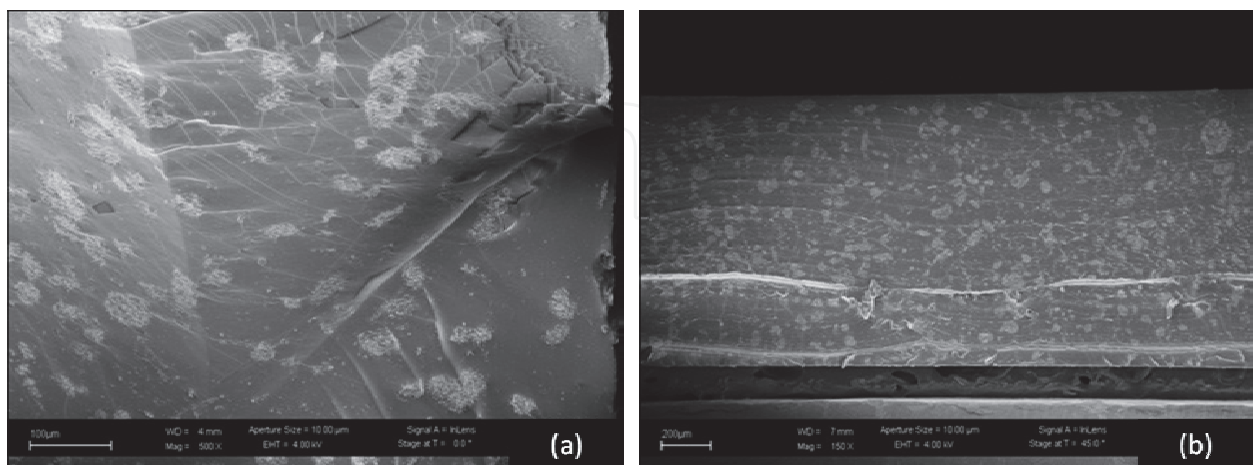


Fig. 4. Using a sonicator as an alternative to manual mixing with mortar and pestle gives rise to composites with unsatisfactory dispersion of the filler. Both images refer to 1 wt% composites, with different magnification ratios (a) 100 kx and (b) 200 kx.

The sample (1 wt%) were made similarly to preparation “A” but in lieu of using the mortar, the blending of polymer base and nanotubes first and the subsequent addition of the curing agent were achieved through sonication. The idea of using the mortar to mix the nanocomposites' constituents was basically inspired by this failed attempt.

Another advantage of carrying out the mixing through a mortar concerns the level of affinity between polymer and filler. In any nanocomposite material it is important that the constituents are intimately intertwined and closely connected, so that adequate transfer of loads and the setting up of numerous synergistic effects can take place. According to some publications, it is suggested that PDMS molecules can be absorbed on the nanotube surfaces via hydrophobic non-covalent interactions [Baskaran, 2005; Wang, 2006; Beigbeder, 2008] or PDMS has a good wettability on CNTs due to its low surface tension [Barber, 2004]. Obviously, the higher the degree of dispersion, the more pronounced the affinity between nanotubes and PDMS is. Very magnified images (200÷500 kx) of MWCNTs embedded in the nanocomposite were collected in order to estimate this important aspect. By shooting such magnified images, it was possible to measure the nanotubes' diameters (Figure 5). It was observed that more often than not it exceeded the expected value of ≤ 70 nm, meaning that they must be coated by the polymer which contributes to increase the tubes' diameter.

4. Electrical and thermal transport characterizations

The aim of this paragraph is to report on the electrical and thermal characterization that was performed on PDMS/MWCNT composites with different nanotube concentrations. The conductivities of the nanocomposites were obtained and fitted with a scaling law derived from percolation theory, with a good agreement between theory and experiment. Thermal transport properties were investigated by means of the laser flash technique, which is a powerful tool for the evaluation of the transport properties in solids.

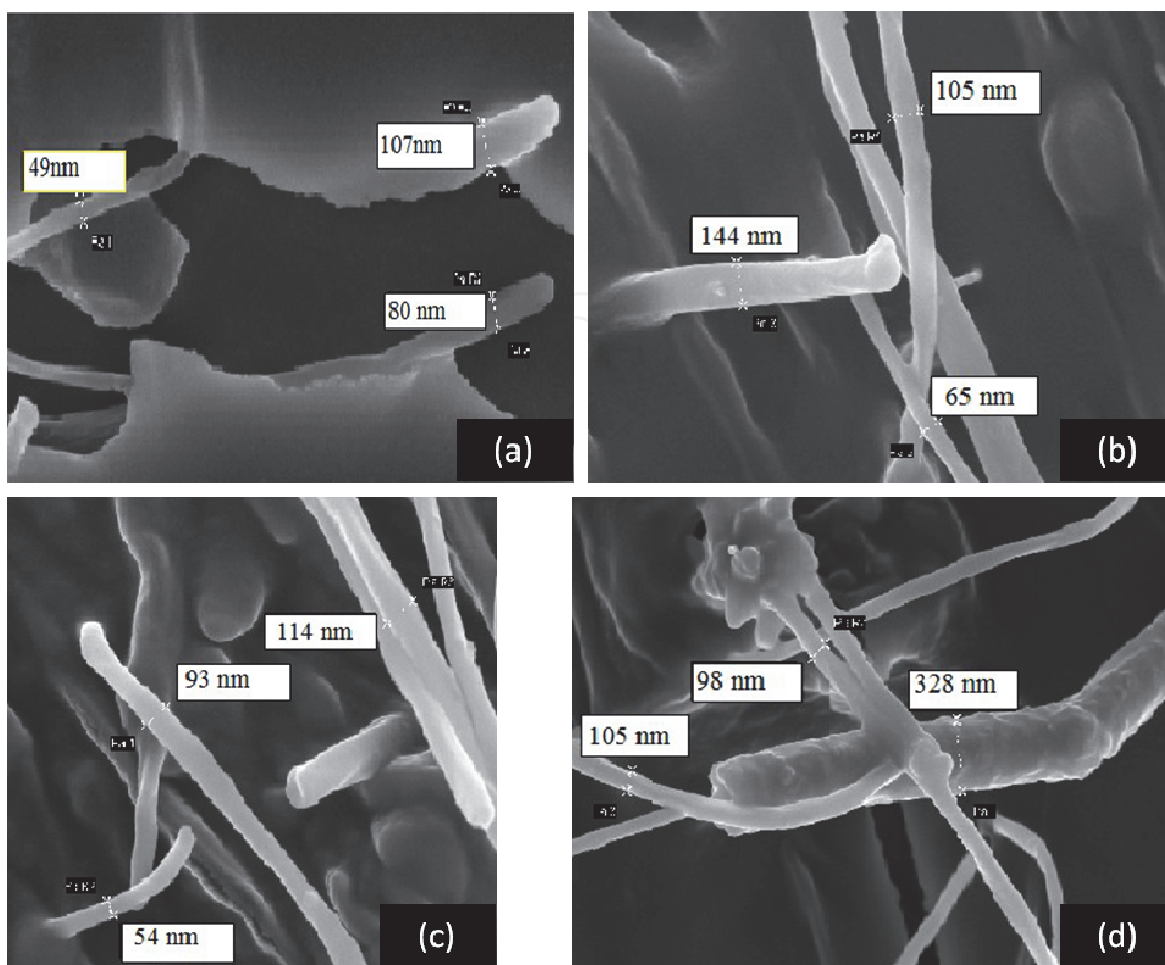


Fig. 5. FESEM images of individual carbon nanotubes belonging to (a) 2 wt% nanocomposite (prep. "A"), (b) 3 wt% nanocomposite (prep. "B"), (c) 4 wt% (prep. "B") and (d) 6 wt% (prep. "B"). According to the specifications of the nanotubes manufacturer, the clean nanotubes' diameter is around 50nm, as expounded in Table 1.

4.1 DC electrical characterization

Electrical transport properties of PDMS/CNT composite were previously reported from several research groups [Liu & Fan, 2007; Bokobza et al, 2008; Khosla & Gray, 2009; Liu & Choi, 2009], with a various range of percolation thresholds p_c 's (between 0.05 wt% and 4 wt%), and this aspect is not contradictory since p_c depends principally on CNT morphological characteristics (i.e. aspect ratio). Some authors report the non-linearity of I-V curves for filler concentrations close to the percolation threshold. C.-X. Liu and J.-W. Choi [Liu & Choi, 2009] observed a parabolic rather than a linear increase of the current density at high voltages. The non-linear behaviour was more conspicuous at low filler loadings. Non-linearity of the I-V characteristic was also argued by C.-H. Liu and S.S. Fan [Liu & Fan, 2007]. The CNTs loadings were in range of 0.1÷3 wt% and the dispersion of MWCNTs was obtained through ball milling and ultra-sonication. The I-V curve for 1 wt% loading displayed a marked nonlinear behaviour. The curve is symmetric and indicates that the resistance depends upon the applied voltage. In a later article the same authors [Hu et al, 2009] showed that the non-linearity of the I-V curve is a feature mostly associated with low concentrations of MWCNTs. For a concentration of filler as low as 0.35 wt%, authors

claimed that the current/voltage curve is symptomatic of the presence of a Schottky contact. The non-linearity of the curve becomes less and less noticeable with increased filler loading, like in the case of the 5 wt% sample. The reasons for the observed nonlinearity may be found in a tunnelling transport theory developed by P. Sheng in 1980 [Sheng, 1980], called fluctuations-induced tunnelling. This theory applies to random systems, such as conductor-insulator composites, disordered semiconductors, or doped organic semiconductors, where the electrical conduction is dominated by electron transfer through tunnelling between conducting segments. The theory may apply to PDMS/MWCNT composites by postulating that carbon nanotubes are coated by the elastomer and electrical transport sets in if the electrons tunnel through the insulating barrier that separated the nanotubes. In this picture of events, those barriers would be lowered by an external voltage, thus accounting for the observed resistance drop.

To correctly perform the electrical measurements (in a four point probe configuration), it is important to avoid a direct pressure on the contacts, avoiding an influence of the piezoresistive behaviour of the material on the global resistivity. In our samples, PDMS/CNT composites were spooned inside hollow parallelepiped-shaped structures formed on the surface of a pure PDMS block; the structures on the surface were sufficiently thin ($\ll 1$ mm) so that the sheet resistance approximation holds. The composites were casted inside the pre-defined geometries and let cross-linked in situ. Metallic electrodes were deposited through thermal evaporation in high vacuum condition: in particular, the electrodes consisted of high aspect ratio conductive strips transversally bridging the composites.

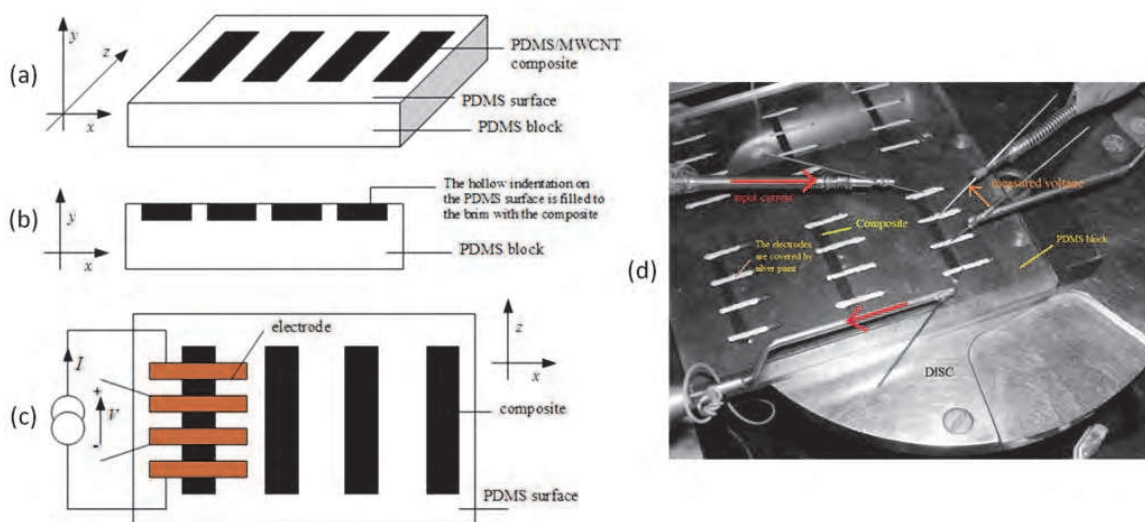


Fig. 6. A schematic diagram that illustrates the premises of the four-terminal sheet resistance measurement of PDMS/MWCNT composites. The key aspect of the new design is shown in (c): four electrodes are deposited on PDMS and on the composite and the four multimeter probes can be placed on the sections that are solely in contact with the elastomer. Picture (d) represents the final system: current is supplied by two probes and voltage drop is detected by the other two central probes. In this way a four-terminal sheet resistance measurement is made for each stripe of PDMS/MWCNT composite.

Contact with the probe is then achieved on one of the two sections that are glued to PDMS. A Ti (5 nm)/Cu (200 nm) bilayer was chosen, Ti acting as adhesion layer. The sample shape and electrical connections are represented in Figure 6.

The PDMS block offers a mere structural role therefore. Its main asset is denoted by its flexibility that confers the elastomer the ability to absorb most of the pressure applied during an I-V measurement, without transmitting it to the PDMS/MWCNT composite that is being analysed. The nanocomposites were prepared with ten different carbon nanotube concentrations: 0.5, 0.7, 1.0, 1.2, 1.5, 2.0 wt% (preparation "A"), 3.0, 4.0, 5.0 and 6.0 wt% (preparation "B"). The uncured composites were cast into the thin structures by filling them to overflowing using a small metallic spatula and then removing the excess material from the stripes by dragging a cutter blade across them. The composites with low nanotube concentrations (<1.5 wt%) were cast into the 500 μm -thick blocks for practical reasons; on the other hand, it was easier to fill the 200 μm -deep structures when dealing with higher concentrations. For each stripe two or more I-V measurements were collected depending on the concentration of carbon nanotubes. For samples with very low concentrations we were able to record voltage drops for a limited current ranges because of their high resistance. The 0.7, 1.0 and 1.2 wt% samples presented non-linear I-V curves, as shown in Figure 7 for the last two CNT concentrations. The curves attain linearity around the origin that is lost for more intense electric currents. However, for nanotubes concentrations exceeding 1.5 wt%, the I-V curves were near perfect straight lines, thus differing from what was ascertained during bulk resistance measurements.

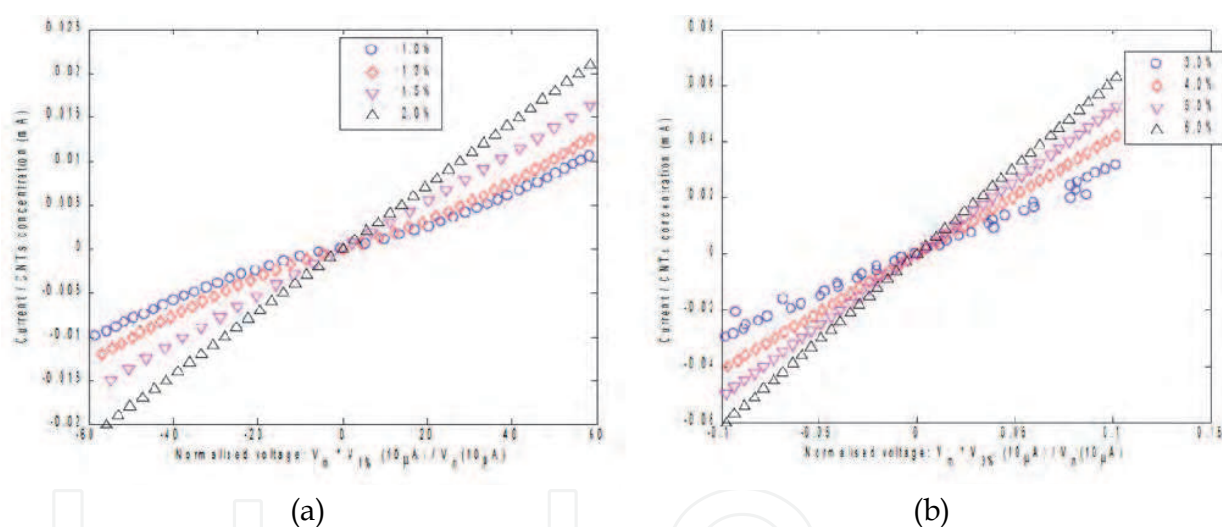


Fig. 7. (a) Normalised I-V curves of four nanocomposites (1.0, 1.2, 1.5 and 2.0 wt%, prep. "A"). The input current was set to cover the range from $-10\mu\text{A}$ to $+10\mu\text{A}$ during the experiment. The curves belonging to the 1.0 wt% and 1.2 wt% composites exhibit linearity around the origin and a parabolic-like trend for intense electric currents. Their differential resistance is not constant, but rather attains a maximum about the origin. (b) Normalised I-V curves for four high-CNT concentrations (prep. "B"). The curves are all linear. For all samples the input current was $[-10,+10]\mu\text{A}$.

Their trends are shown in Figure 7 (a) and (b). In order to represent their values on a common scale, the measured voltages belonging to each composition (V_m in the figures) have been normalised so that they occupy the same tension scale of the 1 wt% sample (Figure 7 (a)) and the 3 wt% sample (Figure 7 (b)). Having the same voltage range, the currents were differed from one percentage to the other by normalising the input values with respect to the CNTs content.

The fluctuations-induced tunnelling model that supposedly governs the electron transport in the composites may still be well-grounded. The fact is that the non-linear behaviour contemplated by the model is present in those nanocomposites with filler concentrations very close to the percolation threshold. But as the nanotube content is increased the insulating barriers that allegedly separate contiguous CNTs are reduced to such an extent that electrons have limited difficulty penetrating them. Our I-V curves tally quite well with what has been reported in literature. Liu and Fan [Liu & Fan, 2007] attributed the observed nonlinearity to the formation of a Schottky-like contact, but this claim seems preposterous in the light of our I-V curves. The electrical characteristic for a Schottky contact is roughly similar to that of a classic p-n junction, which is above all asymmetric about the origin. Our curves, even the non-linear ones, are instead symmetric. The single sheet resistance value was obtained for each stripe and it can then be turned into a bulk resistivity value by virtue of the following equation:

$$\rho = R_{sheet} \frac{d}{d_{el}} w ,$$

where ρ is the bulk resistance, d and w are the width and thickness of the stripes respectively, and d_{el} is the average distance between two electrodes.

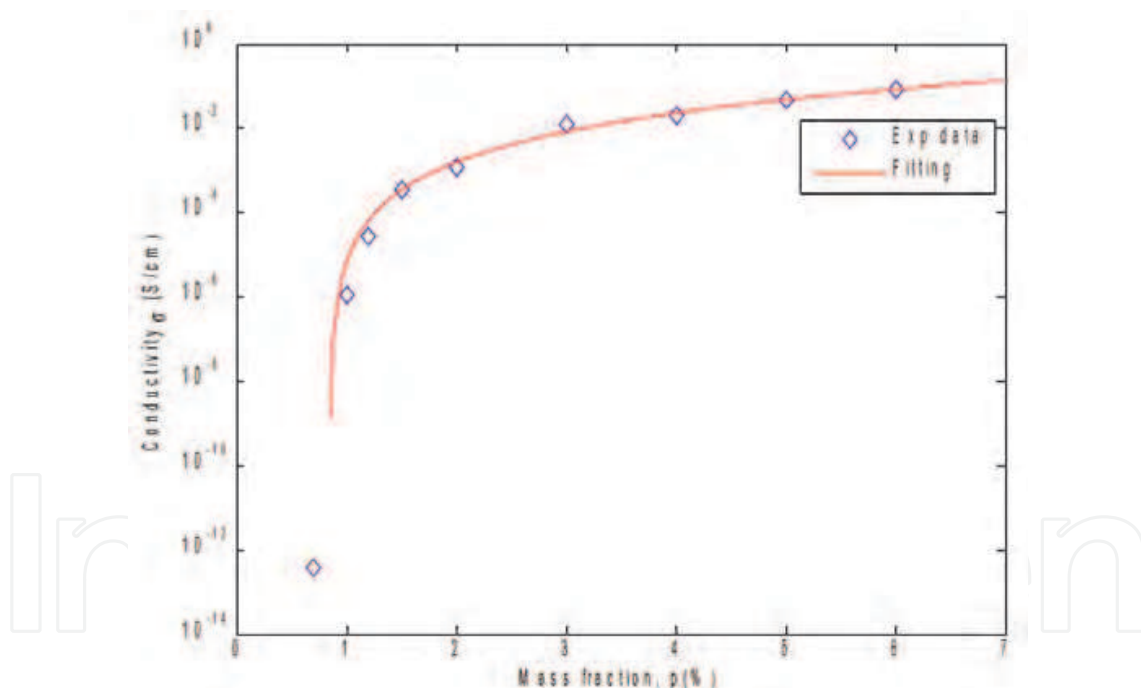


Fig. 8. Conductivity values of the PDMS/MWCNT nanocomposites for different filler concentrations (blue rhombus). Experimental data were fitted with the scaling law from percolation theory (red line). The fitting curve can be expressed as: $\sigma = 1.1 \cdot (p - 0.85)^{2.67}$ mS/cm.

As visually represented in Figure 8, the conductivity jumps up by several order of magnitudes passing from low loadings around the percolation threshold (0.7 and 1.0 wt%) to those above that critical value. The conductivity continues to rise but seemingly its increasing trend gets sluggish for higher concentrations (5.0 and 6.0 wt%). This probably points to the existence of a plateau at higher concentrations, as indeed envisioned by

percolation theory. The data shown in Figure 8 were fitted by the well-known percolation scaling law:

$$\sigma = \sigma_0 (p - p_c)^t,$$

where σ_0 is a proportionality constant, p_c is the percolation threshold, and t is the critical exponent that characterise the percolative network [Stauffer & Aharony, 1994]. The outcome of the fitting delivered the following parameter values:

- $\sigma_0 = 1.1 \text{ mS/cm}$;
- $p_c = 0.85 \%$;
- $t = 2.67$.

According to the percolation theory, the power of the scaling law has the remarkable feature that it is entirely independent of the kind of system being studied, and it only depends on the dimensionality of space. The scaling law and the critical exponent are universal and it is only the percolation threshold that changes according to the percolating system under analysis. Computer simulations on “ideal systems” have all consistently shown that the critical exponent is exactly equal to 2.0. However, more realistic simulations [Stanley, 1977; Kogut & Straley, 1979] have demonstrated that the critical exponent can exceed the universal value of 2.0, with maximum values that are set by a combination of different geometrical factors. Many works in the literature regarding polymer/CNT nanocomposites report t values between 2 and 3 [McLachlan, 2005 and references therein].

4.2 Thermal transport characterization

Thermal transport properties are a crucial characteristic to face in designing disposable biodevices. For instance, the efficiency and selectivity of Polymerase Chain Reaction (PCR) is strictly related to the execution of fast thermal transitions among the three temperatures required by the protocol. Polymeric materials are very promising in the fabrication of biodevices, but their low thermal conductivity is often a bottleneck in the design of highly efficient systems. The development and study of innovative materials and technological processes gained a crucial importance to give life to a new generation of small, portable and fast devices. Polymeric composites, in the case of filling with thermally conducting nanomaterials, can show a dramatic improvement in thermal response with respect to pure polymers. Since the biocompatibility of PDMS is well known, lowering its thermal inertia can open new interesting ways for its widespread application. Some works about that topic were recently published. C.H. Liu et al. [Liu et al, 2004] reported an enhancement of 65% in thermal conductivity with 4 wt% MWCNT loading in the silicone elastomer. The increase in thermal conductivity is nowhere near as dramatic as the enhancement in electrical conductivity. T. Borca-Tasciuc [Borca-Tasciuc, 2007] has argued that heat transport is inefficient owing to the high thermal resistance between neighbouring nanotubes and between nanotubes and the matrix. In order to maximise heat transport, the authors infiltrated the polymer on long, vertically-aligned carbon nanotubes. In this way, the number of tube/polymer interfaces in the direction of charge flowing is minimised. Composites grown in line with this approach will display a significant level of anisotropy as far as thermal properties are concerned in the directions parallel and perpendicular to the aligned nanotubes. Through a photo-thermoelectric technique they inferred that the thermal diffusivities are insensitive in the range of 180÷300 K. Moreover, they found that the thermal

diffusivities in the perpendicular direction are $\sim 2\div 4$ times smaller than in the parallel direction and larger than effective media theory predictions using reported values for the thermal diffusivity of millimetre thick aligned multi-walled carbon nanotube arrays.

Here we report on the thermal transport properties characterization of PDMS/CNT nanocomposite with different filler content by means of the laser flash technique [Parker et al, 1961]. This methodology allows measuring the room temperature thermal diffusivity (α). A pulsed laser (wavelength 1064 nm, energy 3 J, spot area 0.8 mm²) impinged on cylindrical shaped samples with a diameter of 1 cm and a thickness of ~ 1 mm (measured with a Mitutoyo thickness gage, resolution 0.001 mm). Since the polymeric matrix is completely transparent in the IR region, a relatively thick chromium layer was deposited by RF magnetron sputtering on the surface exposed to laser radiation, to guarantee complete adsorption of the impinging energy. Temperature was measured on the opposite side with a thermocouple.

Laser flash characterization results are reported in Figure 9. Data were analyzed following the model proposed by Parker et al. [Parker et al, 1961] that links the thermal diffusivity α with sample thickness L and time $t_{1/2}$ required for the back surface to reach half of the maximum temperature rise:

$$\alpha = 1.38 \frac{L^2}{\pi^2 t_{1/2}}$$

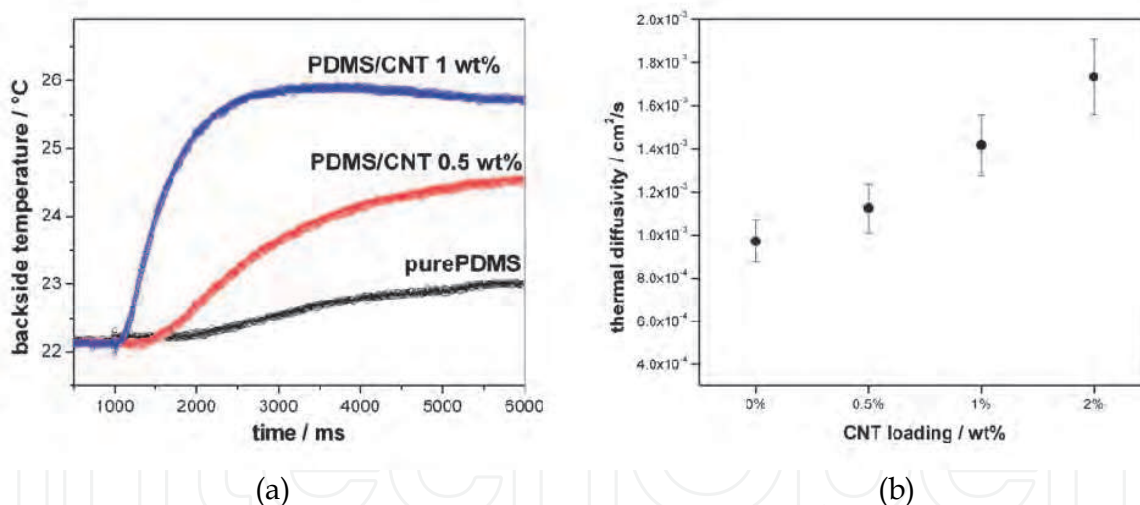


Fig. 9. (a) Raw data obtained by laser flash measurements for pure PDMS and PDMS/CNT composites with 0.5 and 1 wt% CNT loading. (b) Thermal diffusivities for pure PDMS and PDMS/CNT nanocomposites with 0.5, 1 and 2 wt% filler content.

The improved thermal response is evident both in the raw curves and on the thermal diffusivity evaluations. It emerges that a $\sim 50\%$ enhancement in α value can be achieved with a 1 wt% nanotube charging. This result is perfectly compatible with the evaluation previously reported by Borca-Tasciuc et al. [Borca-Tasciuc, 2007], since the 1.25 times increase in heat transport evaluated perpendicularly to the axis of the tubes is due to the entangled tubes, similarly to what happens in our isotropic system. A significant improvement can therefore be noticed, even with a very low filler loading.

5. Nanocomposite application for the fabrication of a stationary PCR biodevice

Recently we proposed the application of the PDMS/CNT nanocomposite for the fabrication of a miniaturized device for the Polymerase Chain Reaction for DNA amplification [Quaglio et al, 2011]. We demonstrated that the better thermal behaviour for devices made of the nanocomposite material with respect to the one made of pure PDMS allowed faster temperature transitions and a better control in steady-state temperatures. The better thermal performance of the nanocomposite-based device was mirrored by an efficiency increase in PCR reaction, demonstrating the direct enhancing effect of the CNTs content in the composite.

An example of the fabricated device is reported in Figure 10. A LOC with a non-symmetric drop-like shape was designed (volume 15 μl , including inlet and outlet cylinders), to optimize the contact between the chamber surfaces and the liquids, avoiding air bubbles formation. The reaction chamber was bonded to a silicon substrate with a thin film (approximately 100 μm thick) of the same nanocomposite, to guarantee the fluidic structure sealing.

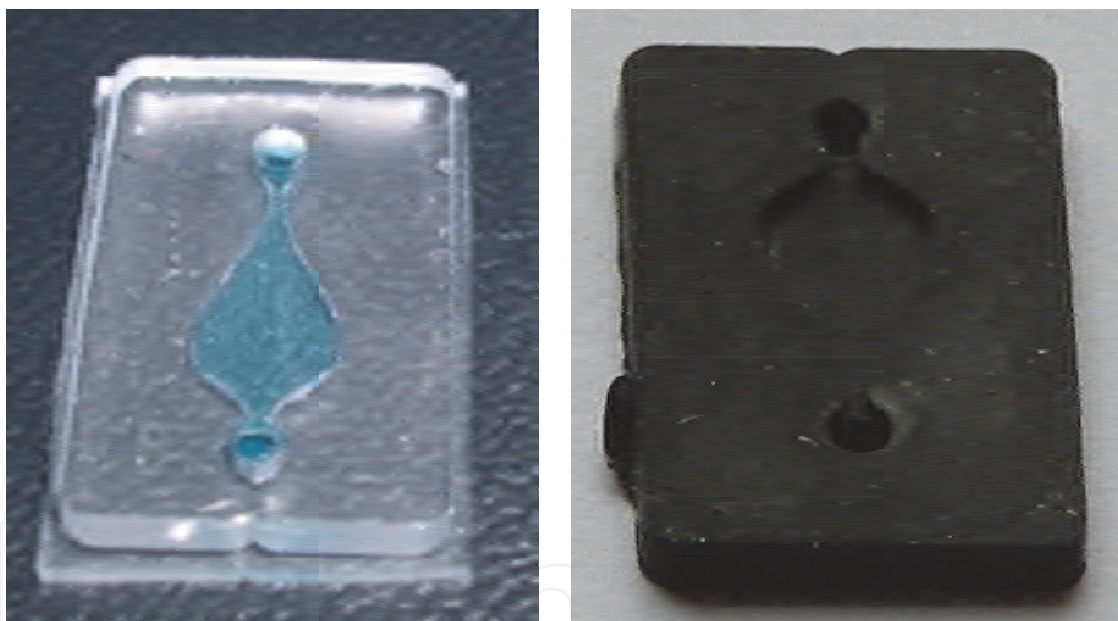


Fig. 10. Example of chips used for PCR protocols.

To estimate the thermal response on LOC device, the temperature profile during standard PCR thermocycling was evaluated directly on-chip. Temperature was measured with a thermocouple, inserted into the device close to the reaction chamber, but completely surrounded by the material, to minimize any external effect on the thermal response. On-chip thermal profiles are reported in Figure 11. We clearly observed a faster transition and a better control in steady-state temperatures when using the nanocomposite and while increasing the CNTs loading.

The performance of PDMS and PDMS/CNT LOCs was evaluated by the detection of PCR products related with the Human Actin Gene with a length of 150 base-pairs (bp) and with a different PCR protocol related with the Human β -Actin with a length of 756 bp. Details

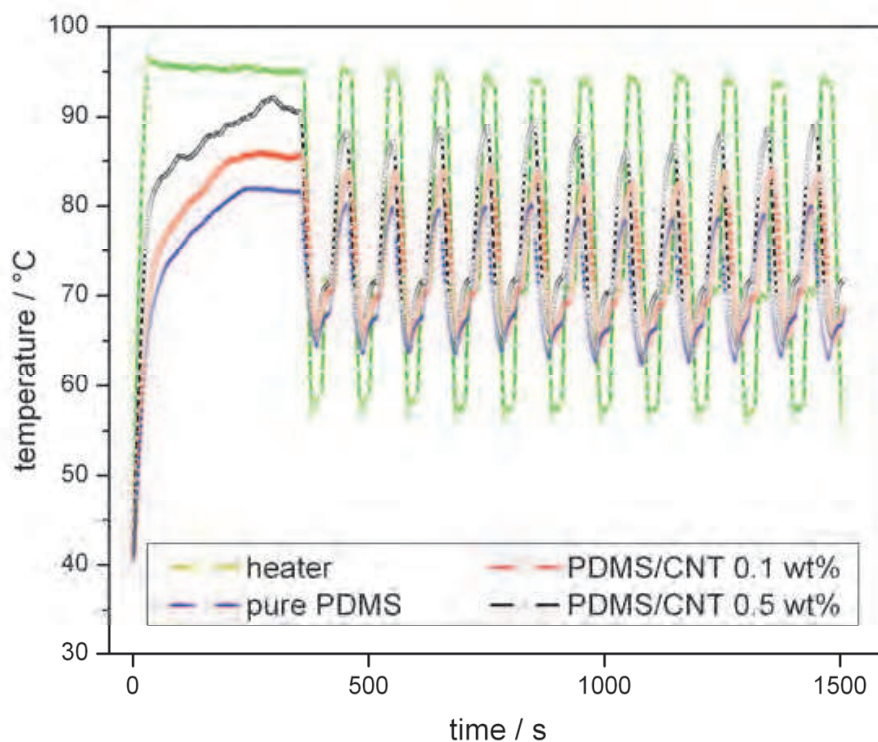


Fig. 11. Evaluation of the on-chip thermal profile during a standard PCR thermocycling, both for pure PDMS and for nanocomposites with different filler loading.

about the biological protocols are reported elsewhere [Marasso et al, 2011; Quaglio et al, 2011]. For both biological models, the PCR standard thermal protocol consisted on 5 min for pre-denaturing at 95 °C, 20 s for denaturing at 95 °C, 20 s for annealing at 55 °C, 20 s for extension at 72 °C repeated for 40 cycles, and finally a post-extension at 72 °C for 2 min. To enhance the effect of the improved thermal diffusivity of the nanocomposite, we designed a shortened protocol to allow stopping the fragment amplification during the exponential phase. Therefore, on the modified protocol the denaturing, annealing and extension steps were shortened to 10 s, the number of cycles was set to 20 and the final post-extension step was deleted.

The PCR products were analyzed by a 3% agarose gel (A5093, Sigma), electrophoresis separation stained by ethidium bromide (Sigma) and then visualized under UV light. The DNA Ladder used was the GeneRuler™ 100 base-pairs (SM0243, Fermentas). The pictures of the loaded agarose gels were analyzed with GelAnalyzer, a freeware 1D gel electrophoresis image analysis software.

Standard thermal protocol is designed for optimal PCR response in pure PDMS device. Following such protocol, PCR reaction reaches its saturation point and reaction efficiency can be evaluated from the intensity in the agarose gel picture. In other words, thermocycling is so slow to allow PDMS to reach sufficiently high temperature to permit the reaction to be efficiently performed. If the same protocol is applied to nanocomposite-based chip, exactly the same efficiency is noticed, because in both cases (on PDMS and PDMS/CNTs samples) the reactions reach the saturation plateau (and our experimental output is only related with the end-point result of the reaction). The standard protocol was used to estimate the

maximum amount of amplicons concentration. To emphasize the improvement in reaction efficiency related to the improved thermal behaviour, it is mandatory to design a shortened protocol, to stop the fragment amplification during its exponential duplication and before the achievement of the plateau (the PCR phase defined as the attenuation in the rate of the exponential product accumulation) which is seen concomitantly in later PCR cycles [Kainz, 2000]. In such case, the faster transition for nanocomposite chip is expected to play a determining role in the end-point reaction output, with a significant difference with respect to what evaluated for pure PDMS chip.

Four PCR tests were performed using standard protocol, revealing a similar and reproducible concentration (Standard PCR tubes: (9.9 ± 0.2) g/l; PDMS: (9.8 ± 0.3) g/l; PDMS/CNT: (10.1 ± 0.2) g/l). Afterwards, standard PCR tubes and both PDMS and PDMS/CNT LOCs were tested in quadrupole with the shortened protocol. The agarose gel pictures reported in Figure 12 (a) indicated a DNA concentration of (9.9 ± 0.2) g/l for standard PCR tubes, (9.8 ± 0.1) g/l for the PDMS/CNT LOC and (7.6 ± 0.2) g/l for the PDMS LOC. Assuming that the concentration achieved with the standard protocol (10 g/l) was the maximum result for our bio-design, we estimated the relative efficiency of the PCR reactions. As reported in Figure 12 (c), while the DNA amplification for the shortened protocols on PDMS/CNTs LOC (97.6%) was comparable with the maximum value obtained with standard PCR tubes (98.7%), it was sensibly reduced on PDMS LOC (75.3%).

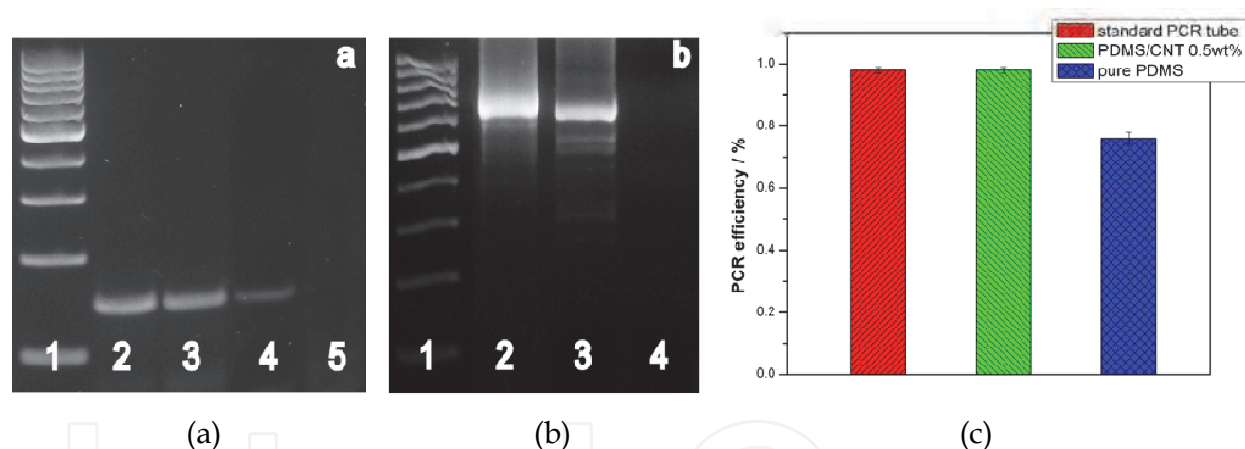


Fig. 12. (a) 3% agarose gel image: (1) 100 bp DNA Ladder (2) PCR amplicon obtained with standard PCR tube (3) PCR amplicon obtained with PDMS/CNT 0.5 wt% LOC (4) PCR amplicon obtained with PDMS LOC (5) negative control. (b) 3% agarose gel image: (1) 100 bp DNA Ladder (2) PCR amplicon obtained with PDMS/CNT 0.5 wt% LOC (3) PCR amplicon obtained with PDMS LOC (4) negative control. (c) Results of PCR reaction with shortened protocol. Efficiency equal to 1 is considered for PCR standard thermal protocol.

A subsequent test performed with the PCR protocol for Human β -Actin (756 bp) allowed evaluating the presence of non specific or uncompleted DNA sequences. As reported in Figure 12 (b), both LOC devices confirmed their performances concerning the amount of PCR production. Otherwise, while PDMS/CNT LOC devices showed no presence of nonspecific amplicons, the PDMS LOC revealed shorten non-specific amplicons.

With the reported experiments we were able to conclude that the PCR can be performed in nanocomposite-based chips with low filler content with a 25% improvement in reaction

efficiency, without noting any non-specific duplication or enzyme segregation. In other words, a 75% reduction in reaction time can be applied without compromising the reaction efficiency.

5. Conclusions

Nanocomposite materials have generated considerable interest over the last few years and their number as well as their field of employment is predicted to rise. Among them, polydimethylsiloxane/carbon nanotube composites have only recently been investigated and the material has displayed a variety of properties that may be exploited in promising MEMS applications and biodevice fabrication. In this chapter we tried to give a general overview on the application reported recently in literature, trying to underline the possible future application and evolution of the studies. In our mind, the peculiar properties of the material were not completely fulfilled up to now, thus a huge amount of innovative applications still have to be developed. For instance, we would like to mention the possible application in energy harvesting (fully exploiting its photomechanical properties) and on the fabrication of all-polymeric biodevices based on the Electrowetting-On-Dielectrics model. These are the topics currently under evaluation in our research group and we are confident that some interesting results will be rapidly reached.

6. Acknowledgements

Authors would like to thank Nano Carbon Technologies Co Ltd (Japan) for nanotube supply. Moreover, the aid and contribution of Dr. E. Campagnoli, A. Chiodoni and S. Guastella from Politecnico di Torino (Italy) is gratefully acknowledged.

7. References

- Ahir, S.V. & Terentjev, E.M. (2005). Photomechanical actuation in polymer-nanotube composites. *Nature Materials*, 4, (2005), pp. 491-495.
- Ahir, S.V., Squires, A.M., Tajbakhsh, A.R. & Terentjev E. M. (2006). Infrared actuation in aligned polymer-nanotube composites. *Physical Review B*, 73, 8, (2006), pp. 085420_1-12.
- Ajayan, P.M. & Tour, J.M. (2007). Nanotube composites. *Nature*, 447, (2007), pp. 1066-1068.
- Barber, A.H., Cohen, S.R. & Wagner, H.D. (2004). Static and Dynamic Wetting Measurements of Single Carbon Nanotubes. *Physical Review Letters*, 92, 18, (2004), pp. 186103_1-4.
- Baskaran, D., Mays, J.W., & Bratcher, M.S. (2005). Noncovalent and Nonspecific Molecular Interactions of Polymers with Multiwalled Carbon Nanotubes. *Chemistry of Materials*, 17, 13, (2005), pp. 3389-3397.
- Beigbeder, A., Linares, M., Devalckenaere, M., Degée, P., Claes, M., Beljonne, D., Lazzaroni, R. & Dubois P. (2008). CH- π Interactions as the Driving Force for Silicone-Based Nanocomposites with Exceptional Properties. *Advanced Materials*, 20, 5, (2008), pp. 1003-1007.

- Bokobza, L. (2004). Elastomeric Composites. I. Silicone Composites. *Journal of Applied Polymer Science*, 93, 5, (2004), pp. 2095-2104.
- Bokobza, L., Rahmani, M., Belin, C., Bruneel, J.-L. & El Bounia, N.-E. (2008). Blends of Carbon Blacks and Multiwall Carbon Nanotubes as Reinforcing Fillers for Hydrocarbon Rubbers. *Journal of Polymer Science Part B: Polymer Physics*, 46, 18, (2008), pp. 1939-1951.
- Bokobza, L. (2009). Some Issues in Rubber Nanocomposites: New Opportunities for Silicone Materials. *Silicon*, 1, 3, (2009), pp. 141-145.
- Borca-Tascuic, T., Mazumder, M., Son, Y. Pal, S.K., Schadler, L.S. & Ajayan, P.M. (2007). Anisotropic Thermal Diffusivity Characterization of Aligned Carbon Nanotube-Polymer Composites. *Journal of Nanoscience and Nanotechnology*, 7, 4-5, (2007), pp. 1581-1588.
- Chung, D.D.L. (2010). *Composite Materials, Science and Applications* (2nd edition), Springer, ISBN 9781848828308, London.
- Clarson, S.J. & Semlyen, J.A. (1993). *Siloxane Polymers*, Englewood Cliffs, ISBN 0138163154, New York.
- Demir, M.M., Menciloglu, Y.Z. & Erman, B. (2005). Effect of filler amount on thermoelastic properties of poly(dimethylsiloxane) networks, *Polymer*, 46, 12, (2005), pp. 4127-4134.
- Engel, J., Chen, J., Chen, N., Pandya, S. & Liu, C. (2006). Multi-Walled Carbon Nanotube Filled Conductive Elastomers: Materials and Application to Micro Transducers. *Proceedings of the 19th IEEE International Conference on Micro Electro Mechanical Systems*, ISBN 0-7803-9475-5, Istanbul, Turkey.
- Franta, I. (1988). *Elastomers and rubber compounding materials*, Elsevier, ISBN 0444429948, Amsterdam.
- Harris, P.J.F. (2009). *Carbon Nanotube Science*, Cambridge University Press, ISBN 9780521828956, Cambridge.
- Hillborg, H. & Gedde, U.W. (1999). Hydrophobicity Changes in Silicone Rubbers. *IEEE Transactions on Dielectrics and Electrical Insulation*, 6, 5, (1999), pp. 703-717.
- Hu, C.H., Liu, C.H., Chen, L.Z., Peng, Y.C. & Fan, S.S. (2008). Resistance-pressure sensitivity and a mechanism study of multiwall carbon nanotube networks/poly(dimethylsiloxane) composites. *Applied Physics Letters* 93, 3, (2008), pp. 033108_1-3.
- Kainz, P. (2000). The PCR plateau phase – towards an understanding of its limitations. *Biochimica et Biophysica Acta (BBA) - Gene Structure and Expression*, 1494, 1-2, (2000), pp. 23-27.
- Kang, I., Schulz, M.J., Kim, J.H., Shanov, V. & Shi, D. (2006). A carbon nanotube strain sensor for structural health monitoring. *Smart Materials and Structures*, 15, 3, (2006), pp. 737-748.
- Kim, J., Chaudhury M.K. & Owen, M.J. (1999). Hydrophobicity Loss and Recovery of Silicone HV Insulation. *IEEE Transactions on Dielectrics and Electrical Insulation*, 6, 5, (1999), pp. 695-702.
- Kim, Y.A., Hayashi, T., Endo, M., Kaburagi, Y., Tsukada, T., Shan, J., Osato, K. & Tsuruoka, S. (2005). Synthesis and structural characterization of thin multi-walled carbon

- nanotubes with a partially faceted cross section by a floating reactant method. *Carbon*, 43, 11, (2005), pp. 2243-2250.
- Khorasani, M.T., Mirzadeh, H. & Kermani, Z. (2005). Wettability of porous polydimethylsiloxane surface: morphology study. *Applied Surface Science*, 242, 3-4, (2005), pp. 339-345.
- Khosla, A. & Gray, B.L. (2009). Preparation, characterization and micromolding of multi-walled carbon nanotube polydimethylsiloxane conducting nanocomposite polymer. *Materials Letters*, 63, 13-14, (2009), pp. 1203-1206.
- Kogut, P.M. & Straley, J.P. (1979). Distribution-induced non-universality of the percolation conductivity exponents. *Journal of Physics C: Solid State Physics*, 12, 11, (1979), pp. 2151-2160.
- Kovacs, G.T.A. (1998). *Micromachined Transducers SourceBook*, McGraw-Hill, ISBN 0072907223, Boston.
- Lavielle, L. & Schultz, J. (1985). Surface properties of graft polyethylene in contact with water. *Journal of Colloid and Interface Science*, 106, 2, (1985), pp. 438-445.
- Liu, C.H., Huang, H., Wu, Y. & Fan, S.S. (2004). Thermal conductivity improvement of silicone elastomer with carbon nanotube loading. *Applied Physics Letters*, 84, 21, (2004), pp. 4248-4250.
- Liu, C.H. & Fan, S.S. (2007). Nonlinear electrical conducting behavior of carbon nanotube networks in silicone elastomer. *Applied Physics Letters*, 90, 4, (2007), pp. 041905_1-3.
- Liu, C.-X. & Choi, J.-W. (2009). Patterning conductive PDMS nanocomposite in an elastomer using microcontact printing. *Journal of Micromechanics and Microengineering*, 19, (2009), pp. 085019_1-7.
- Lu, S. & Panchapakesan, B. (2005). Optically driven nanotube actuators. *Nanotechnology*, 16, 11, (2005), pp. 2548-2554.
- Lu, S. & Panchapakesan, B. (2006). Nanotube micro-optomechanical actuators. *Applied Physics Letters*, 88, (2006), pp. 253107_1-3.
- Lu, S. & Panchapakesan, B. (2007). Photomechanical responses of carbon nanotube/polymer actuators. *Nanotechnology*, 18, 30, (2007), pp. 305502_1-8.
- Marasso, S.L., Giuri, E., Canavese, G., Castagna, R., Quaglio, M., Ferrante, I., Perrone D. & Cocuzza, M. (2011). A multilevel Lab on chip platform for DNA analysis. *Biomedical Microdevices*, 13, 1, (2011), pp. 19-27.
- Matthews, F.L. & Rawlings, R.D. (1999). *Composite Materials: Engineering and Science*, CRC Press, ISBN 0-8493-0621-3, Cambridge.
- McDonald, J.C. & Whitesides, G.M. (2002). Poly(dimethylsiloxane) as a Material for Fabricating Microfluidic Devices. *Accounts of Chemical Research*, 35, 7, (2002), pp. 491-499.
- McLachlan, D.S., Chitame, C., Park, C., Wise, K.E., Lowther, S.E., Lillehei, P.T., Siochi, E.J. & Harrison, J.S. (2005). AC and DC percolative conductivity of single wall carbon nanotube polymer composites. *Journal of Polymer Science Part B: Polymer Physics*, 43, 22, (2005), pp. 3273-3287.
- Moniruzzaman, M., Chattopadhyay, J., Billups, W.E. & Winey, K.I. (2007). Tuning the Mechanical Properties of SWNT/Nylon 6,10 Composites with Flexible Spacers at the Interface. *Nano Letters*, 7, 5, (2007), pp. 1178-1185.

- Musso, S., Giorcelli, M., Pavese, M., Bianco, S., Rovere, M. & Tagliaferro, A. (2008). Improving macroscopic physical and mechanical properties of thick layers of aligned multiwall carbon nanotubes by annealing treatment. *Diamond and Related Materials*, 17, 4-5, (2008), pp. 542-547.
- Okawa, D., Pastine, S.J., Zettl, A. & Fréchet, J.M.J. (2009). Surface Tension Mediated Conversion of Light to Work. *Journal of the American Chemical Society*, 131, 15, (2009), pp. 5396-5398.
- Parker, W.J., Jenkins, R.J., Butler, C.P. & Abbott, G.L. (1961). Flash Method of Determining Thermal Diffusivity, Heat Capacity, and Thermal Conductivity. *Journal of Applied Physics*, 32, 9, (1961), pp. 1679-1684.
- Quaglio, M., Bianco, S., Castagna, R., Cocuzza, M. & Pirri, C.F. (2011). Elastomeric nanocomposite based on carbon nanotubes for Polymerase Chain Reaction device. *Microelectronic Engineering*, (2011), doi:10.1016/j.mee.2011.01.032.
- Reyes, D.R., Iossifidis, D., Auroux, P.A. & Manz, A. (2002). Micro Total Analysis Systems. 1. Introduction, Theory, and Technology. *Analytical Chemistry*, 74, 12, (2002), pp. 2623-2636.
- Sheng, P. (1980). Fluctuation-induced tunneling conduction in disordered materials. *Physical Review B*, 21, 6, (1980), pp. 2180-2195.
- Stanley, H.E. (1977). Cluster shapes at the percolation threshold: and effective cluster dimensionality and its connection with critical-point exponents. *Journal of Physics A: Mathematical and General*, 10, 11, (1977), L211.
- Stauffer, D. & Aharony, A. (1994). *Introduction to Percolation Theory*. Taylor and Francis, ISBN 0748400273, London.
- Tobolsky, A.V. (1960). *Properties and Structure of Polymers*, Wiley, New York.
- Wang, T., Hu, X., Qu, X. & Dong, S. (2006). Noncovalent Functionalization of Multiwalled Carbon Nanotubes: Application in Hybrid Nanostructures. *Journal of Physical Chemistry B*, 110, 13, (2006), pp. 6631-6636.
- Wu, C.-L., Li, H.-C., Hsu, J.-S., Yip, M.-C. & Fang, W.. (2009). Static and dynamic mechanical properties of polydimethylsiloxane/carbon nanotube nanocomposites, *Thin Solid Films*, 517, 17, (2009), pp. 4895-4901.
- Wu, J., Cao, W., Wen, W., Chang, D.C. & Sheng, P. (2009) Polydimethylsiloxane microfluidic chip with integrated microheater and thermal sensor. *Biomicrofluidics*, 3, 1, (2009), pp. 012005_1-7.
- Xia, Y. & Whitesides, G.M. (1998). Soft Lithography. *Angewandte Chemie International Edition*, 37, 5, (1998), pp. 550-575.
- Xu, J., Razeeb, K.M. & Roy, S. (2008). Thermal Properties of Single Walled Carbon Nanotube-Silicone Nanocomposites. *Journal of Polymer Science Part B*, 46, 17, (2008), pp. 1845-1852.
- Xu, W.J., Kranz, M., Kim, S.H. & Allen, M.G. (2010). Micropatternable elastic electrets based on a PDMS/carbon nanotube composite. *Journal of Micromechanics and Microengineering*, 20, (2010), pp. 104003_1-7.
- Yakobson, B.I., Brabec, C.J. & Bernholc, J. (1996). Nanomechanics of Carbon Tubes: Instabilities beyond Linear Response. *Physical Review Letters* 76, 14 (1996), pp. 2511-2514.

- Zhang, C., Xing, D. (2007). Miniaturized PCR chips for nucleic acid amplification and analysis: latest advances and future trends. *Nucleic Acids Research*, 35, 13, (2007), pp. 4223–4237.
- Zhang, C., Xu, J., Ma, W. & Zheng, W. PCR microfluidic devices for DNA amplification. *Biotechnology Advances*, 24, 3, (2006), pp. 243-284.

IntechOpen

IntechOpen



Carbon Nanotubes - From Research to Applications

Edited by Dr. Stefano Bianco

ISBN 978-953-307-500-6

Hard cover, 358 pages

Publisher InTech

Published online 20, July, 2011

Published in print edition July, 2011

Since their discovery in 1991, carbon nanotubes have been considered as one of the most promising materials for a wide range of applications, in virtue of their outstanding properties. During the last two decades, both single-walled and multi-walled CNTs probably represented the hottest research topic concerning materials science, equally from a fundamental and from an applicative point of view. There is a prevailing opinion among the research community that CNTs are now ready for application in everyday world. This book provides an (obviously not exhaustive) overview on some of the amazing possible applications of CNT-based materials in the near future.

How to reference

In order to correctly reference this scholarly work, feel free to copy and paste the following:

Stefano Bianco, Pietro Ferrario, Marzia Quaglio, Riccardo Castagna and Candido Fabrizio Pirri (2011). Nanocomposites based on elastomeric matrix filled with carbon nanotubes for biological applications, Carbon Nanotubes - From Research to Applications, Dr. Stefano Bianco (Ed.), ISBN: 978-953-307-500-6, InTech, Available from: <http://www.intechopen.com/books/carbon-nanotubes-from-research-to-applications/nanocomposites-based-on-elastomeric-matrix-filled-with-carbon-nanotubes-for-biological-applications>

INTech
open science | open minds

InTech Europe

University Campus STeP Ri
Slavka Krautzeka 83/A
51000 Rijeka, Croatia
Phone: +385 (51) 770 447
Fax: +385 (51) 686 166
www.intechopen.com

InTech China

Unit 405, Office Block, Hotel Equatorial Shanghai
No.65, Yan An Road (West), Shanghai, 200040, China
中国上海市延安西路65号上海国际贵都大饭店办公楼405单元
Phone: +86-21-62489820
Fax: +86-21-62489821

© 2011 The Author(s). Licensee IntechOpen. This chapter is distributed under the terms of the [Creative Commons Attribution-NonCommercial-ShareAlike-3.0 License](https://creativecommons.org/licenses/by-nc-sa/3.0/), which permits use, distribution and reproduction for non-commercial purposes, provided the original is properly cited and derivative works building on this content are distributed under the same license.

IntechOpen

IntechOpen